THE JOURNAL OF PHYSICAL CHEMISTRY B

Article

pubs.acs.org/JPCB

In Situ Characterization of Pharmaceutical Formulations by Dynamic Nuclear Polarization Enhanced MAS NMR

Qing Zhe Ni,[†] Fengyuan Yang,[‡] Thach V. Can,[†] Ivan V. Sergeyev,[§] Suzanne M. D'Addio,[‡] Sudheer K. Jawla,[∥] Yongjun Li,[‡] Maya P. Lipert,[‡] Wei Xu,[‡] R. Thomas Williamson,[‡] Anthony Leone,[‡] Robert G. Griffin,*[,†] and Yongchao Su*[,‡]

[†]Department of Chemistry and Francis Bitter Magnet Laboratory, Massachusetts Institute of Technology, Cambridge, Massachusetts 02139, United States

[‡]Merck Research Laboratories, Merck & Co., Inc., Kenilworth, New Jersey 07033, United States

[§]Bruker BioSpin Corporation, Billerica, Massachusetts 01821, United States

[∥]Plasma Science and Fusion Center, Massachusetts Institute of Technology, Cambridge, Massachusetts 02139, United States

Supporting Information

ABSTRACT: A principal advantage of magic angle spinning (MAS) NMR spectroscopy lies in its ability to determine molecular structure in a noninvasive and quantitative manner. Accordingly, MAS should be widely applicable to studies of the structure of active pharmaceutical ingredients (API) and formulations. However, the low sensitivity encountered in spectroscopy of natural abundance APIs present at low concentration has limited the success of MAS experiments. Dynamic nuclear polarization (DNP) enhances NMR sensitivity and can be used to circumvent this problem provided that suitable paramagnetic polarizing agent can be incorporated into the system without altering the integrity of solid dosages. Here, we demonstrate that DNP polarizing agents can be added in situ during the preparation of amorphous solid dispersions (ASDs) via spray drying and hot-melt extrusion so that ASDs can be examined during drug development. Specifically, the dependence of DNP enhancement on sample composition, radical concentration, relaxation properties of the API and excipients, types of polarizing agents and proton density, has been thoroughly investigated. Optimal enhancement values are obtained from ASDs containing 1% w/w radical concentration. Both polarizing agents TOTAPOL and AMUPol provided reasonable enhancements. Partial deuteration of the excipient produced 3× higher enhancement values. With these parameters, an ASD containing posaconazole and vinyl acetate yields a 32-fold enhancement which presumably results in a reduction of NMR measurement time by ∼1000. This boost in signal intensity enables the full assignment of the natural abundance pharmaceutical formulation through multidimensional correlation experiments.

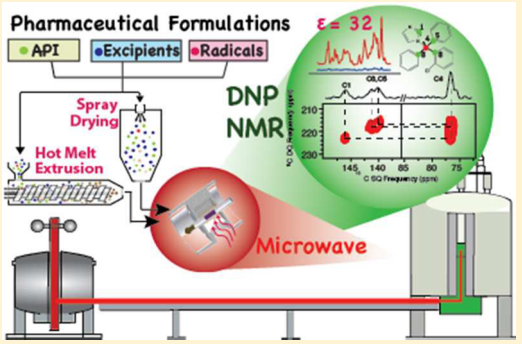

INTRODUCTION

The stability, solubility, and bioavailability of active pharmaceutical ingredients (APIs) are key determining factors of pharmaceutical formulation performance. Drug molecules can undergo undesired phase transformations, such as amorphous and crystalline interconversion, salt formation, and disproportionation induced by chemical, physical, and pharmaceutical processes, transformations that often result in significant alterations in drug bioavailability. As a consequence analysis by differential scanning calorimetry (DSC), thermogravimetric analysis (TGA), powder X-ray diffraction (PXRD), Raman, and mass spectrometry are routinely employed to monitor the physicochemical properties of an API during drug formulation. In addition to these techniques, magic angle spinning (MAS) NMR can shed light on atomic scale molecular structures, quantify various solid-state forms, and probe molecular dynamics and chemical interactions in a nondestructive and noninvasive manner.[1−7] Although powerful, high throughput measurements by MAS are limited due to the inherently low sensitivity. Detection becomes even more challenging in enabled formulations that contain small amounts of poorly soluble API dispersed in a polymeric matrix for enhancing bioavailability. Furthermore, MAS detection on nuclei other than ^{1}H suffers from both the low natural abundance and the low gyromagnetic ratios of ^{13}C and ^{15}N when compared to ^{1}H, making it impractical to perform multidimensional correlation experiments in a reasonable amount of time for exploration of subtle molecular information.

The sensitivity of NMR can be improved by 2−3 orders of magnitude[8−14] by using dynamic nuclear polarization (DNP), which transfers the high polarization of unpaired electrons to nearby nuclei, such as ^{1}H, ^{13}C, and ^{15}N via microwave

Received: July 21, 2017
Revised: July 31, 2017
Published: August 1, 2017

DOI: 10.1021/acs.jpcb.7b07213
J. Phys. Chem. B XXXX, XXX, XXX−XXX

irradiation of the electron−nuclear transitions. The maximum theoretical enhancement factor is given by $\varepsilon_{max} = \gamma_e/\gamma_n = 658$ where γ_e and γ_n are the gyromagnetic ratios of the electron and nuclei, respectively. Thus, even a fraction of this translates into a time saving of months or years, enabling many otherwise infeasible experiments to be performed.[15,16] The recent developments of high-power microwave sources, NMR probes for cryogenic MAS, biradical polarizing agents, and new sample preparation methods, have enabled DNP to be successfully applied to investigate the dynamics and structures of microcrystalline peptides, membrane proteins, amyloid fibrils, natural products, and catalytic materials.[17−29]

Recent studies have demonstrated the considerable potential of DNP in applications to pharmaceutical chemistry.[30−36] The major challenge to successful DNP experiments lies in developing a suitable method of introducing polarizing agents into the sample for optimum signal enhancement without sample disruption. A number of methods for preparing DNP pharmaceutical samples have been reported, including polymer film casting and glass forming methods.[34,37] In addition, Emsley and co-workers have successfully demonstrated an innovative impregnation method on the pharmaceutical formulations with an organic solvent (1,1,2,2-tetrachloroethane) containing polarizing agents.[24] Enhancements in the range of 40−90 were obtained for commercial formulations containing cetirzine dihydrochloride and excipients povidone, magnesium stearate, hypromellose, and lactose. These enhancements allow rapid characterization via one- and two-dimensional MAS spectra of these formulations with drug loading <10%. Very interestingly, molecular contacts between the API and povidone were evident in the $^{1}H-^{15}N$ correlation spectra. However, the use of organic solvents to dissolve radicals and impregnate formulations of interest can result in perturbations of physical and chemical properties of the components in a formulation. Indeed, in a study of theophylline, the impregnation strategy has been found to induce phase conversions that require further improvement for broader application.[36] Beyond this, the use of solvents requires that polarizing agents have significantly different solubility from other components in the formulation, which limits the practical applications. Therefore, it is preferable to avoid solvents when incorporating polarizing agents into the sample.

The formulation of amorphous solid dispersions (ASDs) is desirable since it enhances drug solubility and bioavailability.[38] Therefore, there is a strong need for new tools to monitor and study the chemical and physical stability during the formulation development to ensure a stable product is delivered to the clinic. DNP can play an essential role in enhancing the capacity and efficiency of MAS NMR during early drug development and provide information on the risks related to drug phase changes in ASDs. Therefore, we have designed a protocol for the preparation of DNP samples with the goals of (1) introducing polarizing agents in a noninvasive manner to maintain the integrity of the sample and (2) utilizing intensity enhancement for rapid measurements to inform on formulation development. Our strategy is to evaluate the in situ incorporation of the polarizing agents during the processes of spray drying (SD) and hot-melt extrusion (HME). These two processes are widely applied for preparing ASDs in the pharmaceutical industry. Briefly, in SD, a solution containing API, polymeric excipient, and free radicals, is sprayed against the flow of warm air that rapidly evaporates the solvent and produces a dried powder. In HME, samples are made by mechanically mixing the solid components at elevated temperatures, which creates an intimately combined melt of all the components that is subsequently cooled and milled into a powder.

In our proposed method for sample preparation, the radicals are codissolved or comixed with formulation components for SD and HME processes, respectively. In this report, a clotrimazole-copovidone binary dispersion was used as a model system to investigate the dependence of signal enhancement on the following parameters: concentration and type of polarizing agent, proton density, and ASD methods. The optimized conditions were then adopted to prepare an ASD composed of posaconazole and ^{2}H-vinyl acetate, giving a maximum DNP enhancement of 32. Our results also show no observable structure perturbation or any phase conversion of drug substance. We show that the large signal intensity increase assists in the full assignment of posaconazole resonances from two-dimensional homo- and heteronuclear correlation experiments. To the best of our knowledge, this is the first documented DNP study investigating pharmaceutical formulations prepared by spray drying and hot-melt extrusion.

EXPERIMENTAL SECTION

Materials. Molecular structures of the materials (API's, polymers, and biradical polarizing agents) used in our study are shown in Figure 1. Copovidone Kollidon VA64, an amorphous random copolymer of 1-viny-2-pyrrolidone and vinyl acetate (60:40 mass ratio and 45−70 kDa molecular weight), was obtained from BASF. Vinyl acetate (VA) was purchased from Polymer Source, Inc. The API clotrimazole and posaconazole were products of Spectrum Chemical Inc. and Merck Research Laboratories (MRL), respectively. TOTAPOL[39] and AMUPol[40] are biradical polarizing agents and were both evaluated to enhance MAS NMR signal intensities. TOTAPOL was available from Dynupol, Inc., and AMUPOL was a gift from and Dr. Olivier Ouari and Prof. Paul Tordo (Aix-Marseille Université). Methanol (HPLC grade from Sigma-Aldrich) was used as a solvent for the spray-drying process. All chemicals were used as received.

Sample Preparation. Solid dispersions of all samples were prepared by either spray drying or hot-melt extrusion (Figure 2). In both cases, a binary physical mixture of API and polymer at a desired weight ratio was prepared by blending in a Turbula mixer. The drug loading (API to polymer mass ratio) was 20% in all preparations, except for the 1% (w/w) drug loading of clotrimazole-copovidone ASD reported in the Supporting Information (Figure S1), which showcases the capability of DNP to detect very weak signals. Typically, ∼ 100 g of the mixture was sealed in a 500 mL glass bottle and blended for 1 h at room temperature. The mixture then underwent spray drying or hot-melt extrusion processes as described below. Pure API and polymer samples were made with the same protocol.

Spray drying was conducted on a ProCepT 4M8-TriX Formatrix spray dryer equipped with a 0.6 mm bifluid nozzle. First, a solution of polymer and API in methanol (∼20−40 mg/mL) with the desired amount of radical (0−2% weight ratio in the dried product) was prepared. The solution was then sprayed against a stream of air flowing at 0.4 m^3/min. The solution was fed into the atomizing nozzle at a rate of 5 mL/min and atomized using compressed air at 70 psi. The inlet and outlet temperatures were 353 and 323 K, respectively. The dried powders were collected and stored at room temperature in 10 mL amber glass bottles in a desiccator.

DOI: 10.1021/acs.jpcb.7b07213
J. Phys. Chem. B XXXX, XXX, XXX−XXX

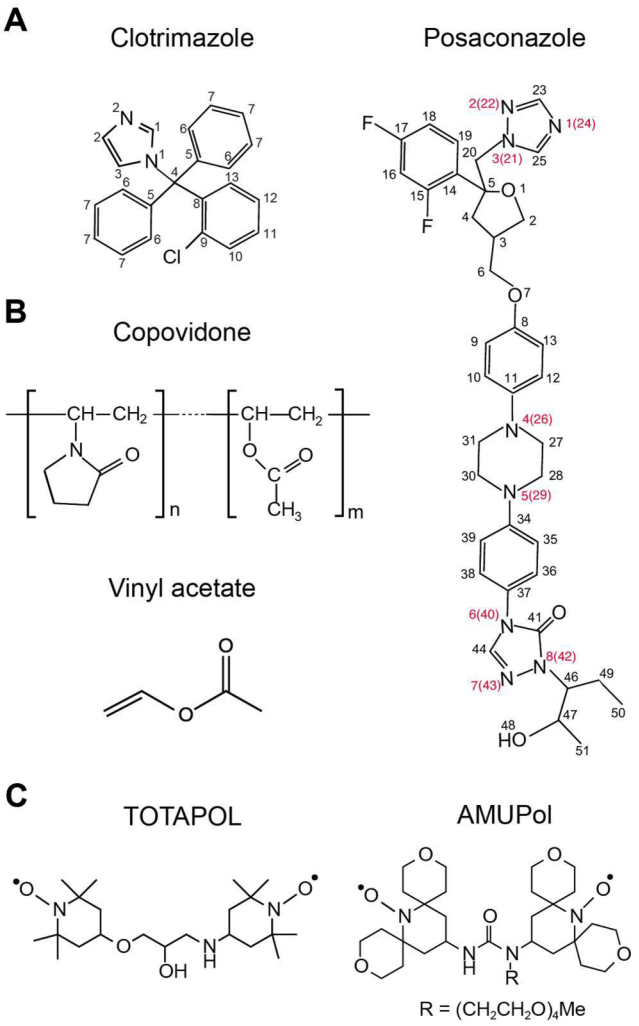

Figure 1. (A) Chemical structures of the two APIs clotrimazole and posaconazole, (B) the polymeric excipients copovidone (n:m = 1:2) and vinyl acetate, and (C) the biradical polarizing agents TOTAPOL and AMUPol. All atoms in clotrimazole and posaconazole are labeled for NMR resonance assignments in the subsequent DNP-enhanced experiments.

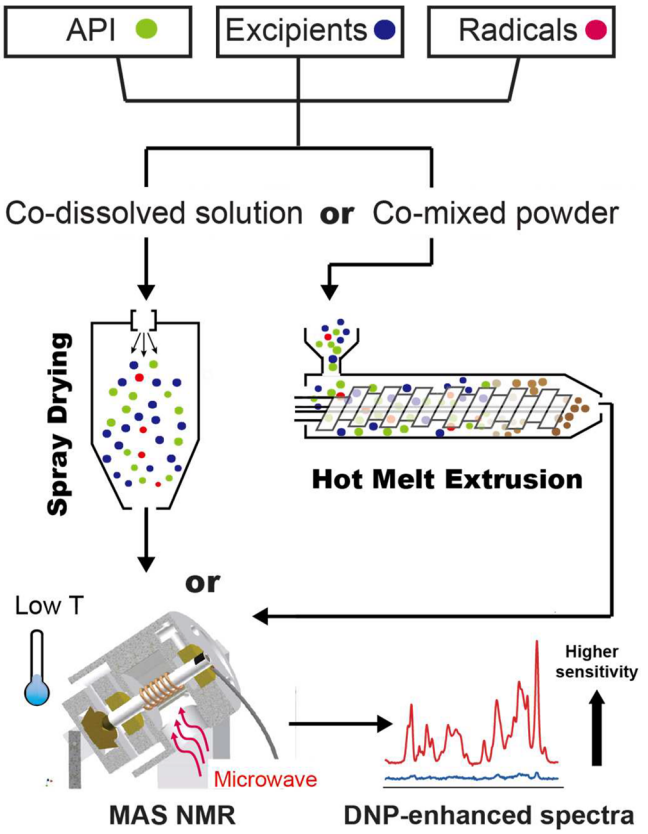

Figure 2. Schematic of amorphous solid dispersions (ASD) sample preparations. Polarizing agents are mixed with the API and polymer molecules in a wet or dry process of spray drying or hot-melt extrusion, respectively. After producing the ASD, the powders can be directly packed for solid-state characterization by DNP-enhanced MAS NMR.

Hot-melt extrusion (HME) was performed with a customized micro twin screw extruder (MP&R Model ME7.5) equipped with corotating conveying screws which have a diameter and length/diameter ratio (L/D) of 7.5 mm and 15:1, respectively.[41,42] In a typical process, ∼ 3 g of the blended binary physical mixture at a desired radical content were fed into the extruder by a vibratory feeder. The barrel temperature was set at 418 K and the screw frequency was 100 rpm. The hot-melt extrudates were collected, allowed to cool, milled into powder via a benchtop mill (Polymix PX-MFC 90 D), and stored in a desiccator at room temperature.

DNP/NMR Experiments. In order to assess the optimum sample condition, $^{1}H-^{13}C/^{15}N$ cross-polarization (CP) experiments were performed on a home-built DNP/NMR instrument operating at 250 GHz/380 MHz with ∼14 W of microwave power.[43,44] Spectra were recorded using a triple resonance (^{1}H, ^{13}C, and ^{15}N) cryogenic MAS probe equipped with a sample exchange system[45] on a home-built NMR spectrometer operating at 9 T at T = 85 K. Approximately 45 mg of each powder sample was packed into a 4 mm sapphire rotor. The spinning frequency is $\omega_r/2\pi$ = 5.5 kHz unless stated otherwise. $\omega_{1H}/2\pi$ = 50 kHz was employed during CP and a TPPM decoupling field $\omega_{1H}/2\pi$ = 100 kHz was used during acquisition. T_{1H} was measured using saturation recovery sequence (Figure S2). Enhancement factors (ε) were calculated by comparing the signals obtained with and without microwave irradiation.

Further characterization by 2D correlation MAS was carried out on a 263 GHz/400 MHz system (consisting of an Avance III HD console, Ascend 9.4 T NMR magnet, and 263 GHz gyrotron) and a 395 GHz/600 MHz system (Avance III HD console, Ascend Aeon 14.1 T magnet, and 395 GHz gyrotron). The microwave power at the sample was ∼10 W on both systems. Approximately 20 mg of each powder sample was packed into 3.2 mm sapphire rotors. At 400 and 600 MHz, $\omega_r/2\pi$ = 9 kHz and 12.5 kHz, respectively. Two kinds of 2D NMR experiments were performed, including $^{13}C-^{13}C$ refocused INADEQUATE (incredible natural abundance double quantum transfer experiment) of clotrimazole and $^{1}H-^{13}C$ and $^{1}H-^{15}N$ HETCOR (heteronuclear correlation) of posaconazole. The refocused INADEQUATE spectra were acquired with a recycle delay of 2 s, 80 t_1 increments, and 384 scans per increment, for a total experiment time of ∼17 h. The HETCOR spectra of posaconazole were acquired with a recycle delay of 3 s, 64 t_1 increments, and 256 scans per increment, for a total experiment time of approximately 14 h. Both short and long contact time (0.45 and 1.5 ms, respectively) HETCOR spectra were acquired to assist with assignments. The sample

DOI: 10.1021/acs.jpcb.7b07213
J. Phys. Chem. B XXXX, XXX, XXX−XXX

temperature during these experiments was 99 ± 2 K, as calibrated using KBr.[46] 2D spectra were processed with zero-filling to double the size and a Gaussian window function centered at 0.1 and 50 Hz of broadening, in both the direct and indirect dimensions. Quadrature detection in the indirect dimension was accomplished using the States-TPPI scheme. All DNP/NMR pulse sequences are included in Figure S2.

RESULTS AND DISCUSSION

Polarizing Agent Concentration. The enhancement and ^{1}H relaxation properties of spray-dried samples with increasing concentrations of TOTAPOL (0, 0.5, 0.75, 1, and 2%, w/w) were measured and are shown in Figure 3. Three different

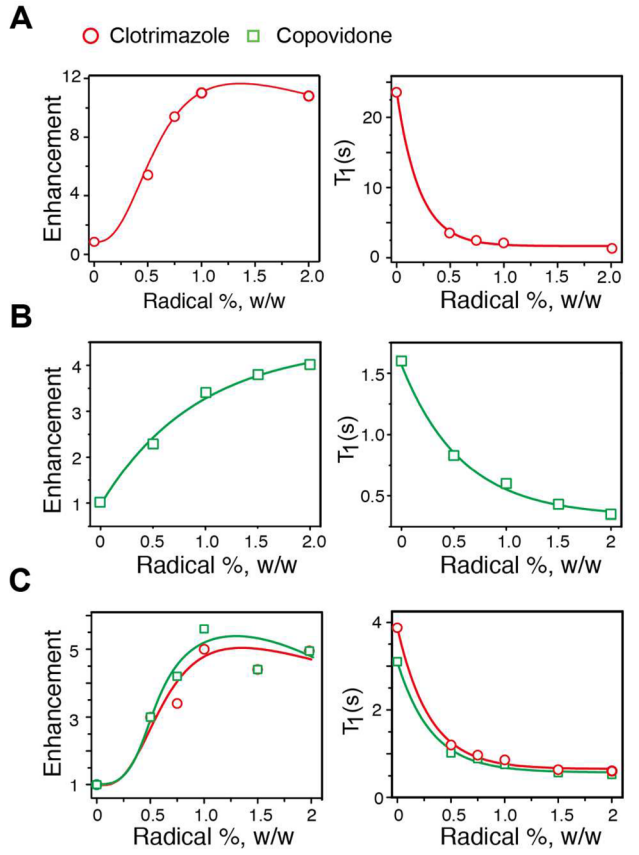

Figure 3. Dependence of DNP enhancement and spin−lattice relaxation property on radical concentration for clotrimazole (A), copovidone (B), and spray dried clotrimazole-copovidone ASD (C). Enhancement and T_1 measurements are shown in the left and right columns, respectively.

sample compositions were used, including pure API clotrimazole (Figure 3A), pure polymer copovidone (Figure 3B), and a clotrimazole/copovidone binary formulation (Figure 3C). We found that for samples containing clotrimazole (Figure 3A and C), the optimal radical concentration was 1%. We note that both SD and HME involve elevated temperatures especially HME (418 K, vide supra), which can potentially lead to thermal degradation of nitroxide radicals. However, the TGA analysis (data not shown) showed that TOTAPOL and AMUPol did not undergo thermal degradation until temperatures of 516 and 526 K, respectively, which is significantly higher than the processing conditions. Furthermore, EPR spectra (Figure S3) share the same characteristics as the published data suggesting that the nitroxides remained intact through the SD and HME processes.[47] EPR spectra also showed no sign of radical aggregation. To evaluate the possibilities of sample perturbations induced by the addition of radicals, we have compared ASDs with and without TOTAPOL using ssNMR and PXRD, shown respectively in Figures S4 and S5. No chemical shift change is observed in the ^{13}C NMR spectra and the X-ray powder pattern also confirms the amorphous nature of the ASDS, suggesting no amorphous to crystalline conversion.

Note also that, to date, DNP applications usually involve solutions of polarizing agents and require 5−10 mM of biradical.[8] The optimum concentration in our method is 2−3 times higher, with 1% weight ratio corresponding to roughly 20 mM of biradical. This may be due to the spatial distribution of the radical in the solid state, where not all radicals are in close proximity to the polymer and/or API.

In Figure 3B, the enhancement of copovidone signal monotonically increased with increasing TOTAPOL and did not saturate at 2% TOTAPOL concentration. We attribute this to polymer motions and hence, the very short T_1 (1.6 s) of ^{1}H in copovidone in the absence of radical. In comparison, pure clotrimazole has much longer T_1 (24 s). However, both components in the clotrimazole/copovidone mixture exhibit essentially the same proton T_1 of ∼3.5 s (Figure 3C), suggesting a good miscibility of the components, which is an indicator of stable pharmaceutical formulations.[48] The miscibility is further supported by the fact that the DNP enhancement is uniform throughout the samples regardless of the radical concentration. A good miscibility in a solid-state mixture is required for efficient ^{1}H−^{1}H spin diffusion, which in turn results in a uniform T_1 and DNP enhancement. Thus, the DNP enhancement may be a useful indicator of the miscibility of pharmaceutical formulations. Both the enhancement and T_1 values of the combined dispersion are roughly equal to the weighted arithmetic average of the two individual components, indicating that the nitroxide is evenly distributed among both members.

An optimum radical concentration is determined based on several parameters. On one hand, higher polarizing agent concentrations provide a denser electron pool, which leads to higher enhancement values. On the other hand, the electrons in the nitroxides are paramagnetic species and lead to paramagnetic relaxation enhancement (PRE) effect. This effect shortens the spin−lattice (T_1) and spin−spin relaxation (T_2) times of nearby nuclei. As a consequence, the PRE effect on T_2 leads to line broadening, loss of resolution and the inability to acquire multidimensional NMR experiments that require T_2 for polarization transfer.[45,49] Therefore, the optimal polarizing agent concentration is a balance of maximizing electron to proton polarization transfer while minimizing PRE effects.

Proton Density. We have investigated the impact of proton density by comparing spray dried intermediates containing either protonated or deuterated vinyl acetate (VA). Both samples were loaded with 20% API clotrimazole and 1% TOTAPOL. Deuterated VA resulted in a greater than 3-fold improvement in the DNP enhancement (12 vs 3.6, Figure 4A), similar to the result found previously in other sample preparation methods.[50−52] In experiments based on CP and detection on low gamma nuclei, such as ^{13}C or ^{15}N, the benefit of diluting ^{1}H in the solvent is 2-fold. First, it reduces the ratio between the populations of protons and electrons. Second, diluting the ^{1}H bath lengthens the intrinsic proton T_1 of an

DOI: 10.1021/acs.jpcb.7b07213
J. Phys. Chem. B XXXX, XXX, XXX−XXX

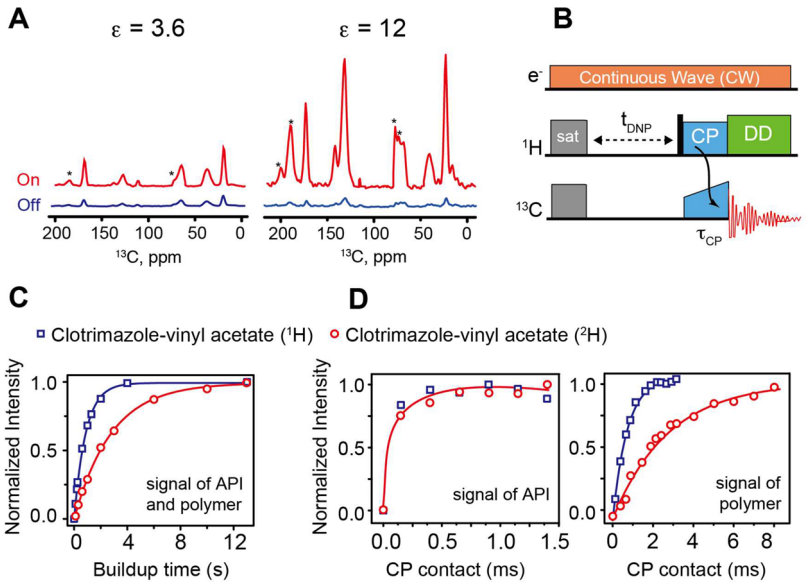

Figure 4. (A) Enhancement spectra of clotrimazole-vinyl solid dispersion samples: ^{1}H vinyl acetate (left) and ^{2}H vinyl acetate (right). (B) Pulse sequence for measuring the dependence of polarization transfer on DNP buildup time, t_{DNP} and CP contact time, τ_{CP}. Build-up curves of DNP (C) and CP (D) for ^{1}H vinyl acetate (blue) and ^{2}H vinyl acetate (red) containing dispersions. In (C), API and polymer exhibit identical t_{DNP}. In (D), CP buildup curves for API and polymer are shown on the left and right, respectively. All data were obtained using 50 kHz of proton spin lock during CP and 100 kHz ^{1}H dipolar decoupling during acquisition at 380 MHz.

undoped sample by attenuating ^{1}H−^{1}H dipole interactions and/or dynamics. The remaining ^{1}H concentration is sufficient to disperse the electron polarization via spin diffusion and transferring that polarization to ^{13}C or ^{15}N via CP. Previous work from Griffin's group has established glass-forming matrix containing glycerol-d_8/D_2O/H_2O (60/30/10, v/v) as a solvent of choice to form a frozen glassy matrix at T < 220 K, and it is used in the majority of DNP biological applications.[50,53] Subsequent studies have explored the use of organic solvents for applications involving insoluble materials; nevertheless, a deuteration level of ∼90% remains standard.[49,54−57] In addition, Akbey et al. obtained a 3−5 fold larger enhancement using perdeuterated then back exchanged SH3 protein instead of protonated samples.[52]

In Figure 4B−D, we study the effect of deuteration on polarization transfer processes during DNP and CP. The pulse sequence for measuring these polarization dynamics is shown in Figure 4B. After saturation (sat) irradiation, the magnetization of protons is enhanced by DNP and then transferred to ^{13}C via CP for detection. DNP buildup curves in Figure 4C showed that the polarization for the protonated vinyl acetate containing sample reached equilibrium at ∼4 s, much faster than that for the deuterated one (∼12 s). This is as expected since protonated polymer has denser ^{1}H matrix for more efficient spin diffusion. As shown in Figure 4D, we observed essentially the same CP buildup curve for the signals from the clotrimazole (left curves in D), whereas signals of protonated and deuterated VA displayed different CP dynamics (right curves in D). Deuterated VA required significantly longer CP contact time (8 ms vs 3 ms) which strongly suggests intermolecular CP from ^{1}H of the API to the ^{13}C of the deuterated polymer. Previously, such information was obtained via ^{1}H−^{1}H and ^{19}F−^{1}H spin diffusion between API and polymer in formulations.[2] Our result opens up a new possibility of obtaining intermolecular contact between API and polymer in pharmaceutical formulations using deuterated polymer excipients.

Hot-Melt Extrusion vs Spray Drying. With the full optimization of DNP enhancement for ASDs prepared via SD, our next goal is to investigate the enhancement performance on dispersions prepared by different techniques. Of particular interest is HME, a low-cost and environmentally friendly method developed over the last three decades for preparing polymer-based ASDs of low solubility drugs. Different from the SD process, where the radical-containing ASD is produced by rapidly evaporating the volatile methanol solvent into hot air and has the advantage of a lower processing temperature which minimizes the thermal degradation of nitroxide radicals, the HME process involves mechanically mixing various ingredients at an elevated processing temperature, thus requiring no solvent and no specific solubility of API, polymer or DNP radical.

Figure 5 compares the DNP enhancement and T_1 relaxation of clotrimazole/copovidone ASDs produced by HME and SD, each with various TOTAPOL concentrations. The HME curve shows that the enhancement reaches a maximum at 0.5% (w/w) radical concentration and remains saturated as the radical concentration is increased, presumably allowing for a greater range of optimal radical concentration than the SD method. Nevertheless, Figure 5B shows that both of these enabled formulation methods yield comparable DNP performances, ε = 5 for clotrimazole/copovidone ASD with 1% TOTAPOL.

HME T_{1H} measurement exhibits a slightly weaker PRE effect on the relaxation at a higher nitroxide concentration in Figure 5C. Due to slower molecular motions at the colder temperatures, T_{1H} values are roughly 4 times longer at cryogenic temperature than at ambient temperatures as shown in Figure 5D. With 1% TOTAPOL (w/w), the T_1 values are approximately 1 s at 107 K for both HME and SD (as reported in Figure 3). The absolute value of T_1 is an indicator of factors, such as particle size, humidity, API-polymer interaction resulting from the dispersion processes as well as the PRE effect. The fact that different processes are suitable for in situ DNP sample preparation diversifies the collection of pharmaceutical compounds and formulations accessible by our

DOI: 10.1021/acs.jpcb.7b07213
J. Phys. Chem. B XXXX, XXX, XXX−XXX

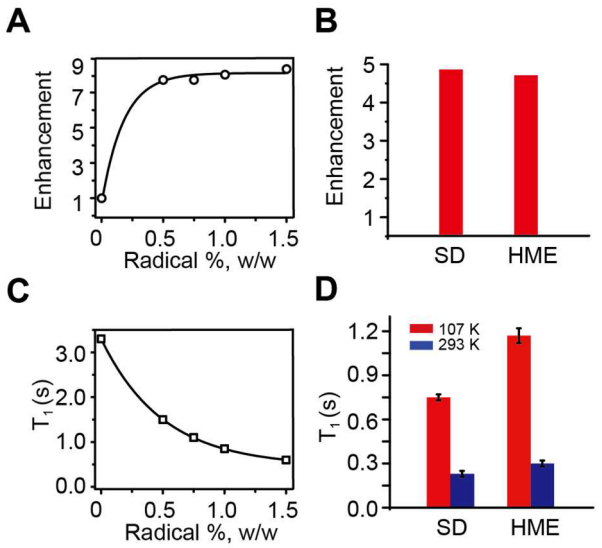

Figure 5. (A) DNP enhancement of extruded clotrimazole/copovidone dispersion with varying (w/w) concentrations of TOTAPOL. (B) Similar enhancement of clotrimazole-copovidone with 1% TOTAPOL prepared via SD and HME. (C) T_1 of the HME samples, measured using a saturated recycle delay value with HC ^{1}H-^{13}C CP experiments with 50 kHz of proton spin lock during CP and 100 kHz ^{1}H decoupling during acquisition at 380 MHz, 90 K. (D) Room temperature (blue) and low temperature (red) T_1 values of clotrimazole-copovidone with 1% TOTAPOL prepared by SD and HME.

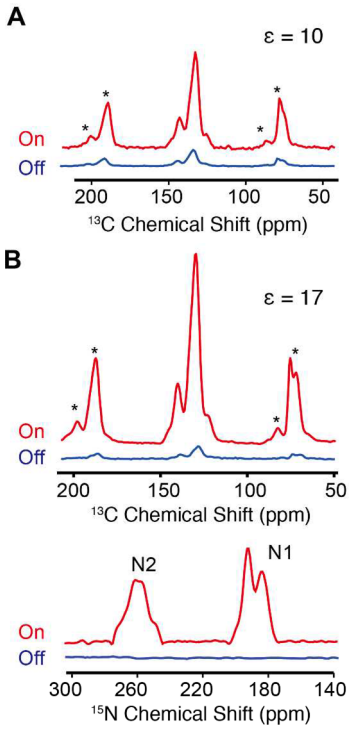

Figure 6. DNP enhanced natural-abundance ^{13}C and ^{15}N CP-MAS spectra showing enhancements of (A) clotrimazole doped with 1% TOTAPOL and at 90 K and (B) 1% AMUPol at 104 K. Enhancements are 10 and 17 at 380 MHz, respectively. The ^{13}C spectra were acquired with 8 scans, recycle delay of 4 s, and the ^{15}N spectrum was collected with recycle delay of 3 s and 8k scans.

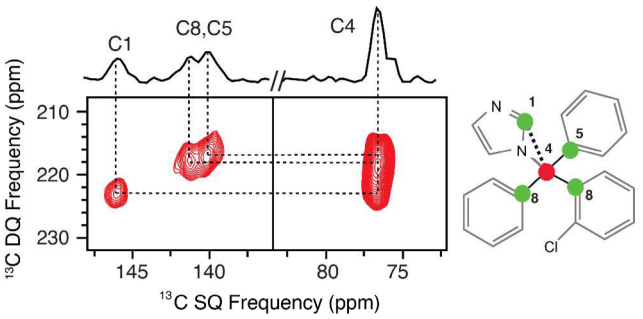

Figure 7. 2D $^{13}C-^{13}C$ refocused INADEQUATE spectrum of clotrimazole showing intramolecular contacts among ^{13}C resonances as marked in the molecular structure on the right. The full spectrum is included in the Figure S4. The 2D spectrum was acquired in 17 h at 106 K on 400 MHz, 384 scans per increment, 2 s recycle delay, and 80 t_1 increments of a 27.7 us.

approach. Overall, the two ASD methods yielded similar DNP performances, suggesting the forgiving nature of introducing polarizing agents in wet and dry manners. Furthermore, it permits selection of the method based on its advantages.

Enabling Multidimensional MAS NMR Spectroscopy for Analyzing Pharmaceutical Formulation. In the previous sections, DNP enhancements of various clotrimazole samples conditions were investigated, including the concentration and types of polarizing agents, proton density, and dispersion techniques. In this section, we present DNP/NMR structural investigations of the samples prepared by the enabled formulation methods. To this end, we first further improved the DNP enhancement by using AMUPol instead of TOTAPOL as the polarizing agent. Figure 6 shows the ^{13}C spectrum of clotrimazole doped with 1% TOTAPOL and ^{13}C, ^{15}N of the same API doped with 1% AMUPol taken at 380 MHz. The enhancement with AMUPol was 17, which roughly doubled that obtained with TOTAPOL. Our result is in good agreement with previous studies that established AMUPol as the radical of choice for DNP applications at ~100 K.[10,40,58] The superior performance of AMUPol facilitates the detection of low natural abundance and low gamma nuclei, such as ^{15}N. In the 1D $^{1}H-^{15}N$ CP of Figure 6, both nitrogen atoms on the imidazole group can be assigned. The doubling of N1 and broadening of N2 suggest that the molecules may adopt two different amorphous forms.[59]

The large improvement in the sensitivity facilitates 2D $^{13}C-^{13}C$ homonuclear correlation experiments as shown in Figure 7. The homonuclear $^{13}C-^{13}C$ spectrum of clotrimazole was acquired using refocused-INADEQUATE, a pulse sequence establishing $^{13}C-^{13}C$ correlations from magnetization transfer through J-couplings.[24,33,60,61] In Figure 7, correlations of C4 with C1, C5, C8 are identified based on previous assignments. The contacts between aromatic carbons are shown in the full 2D refocused-INADEQUATE in Figure S6. The optimized parameters provide a successful example of investigating intramolecular carbon−carbon correlations of natural abundant drugs using DNP-enhanced MAS NMR.

These optimized sample conditions (vide supra) were also applied to the study of the commercialized drug posaconazole, which is a triazole antifungal drug (trade name Noxafil).[62,63] An ASD containing the API posaconazole and polymeric excipient ^{2}H-vinyl acetate with 1% AMUPol was prepared via spray drying. The DNP-enhanced ^{13}C spectra are shown in Figure 8. An enhancement of 25 was obtained for the posaconazole ASD, determined from the microwave-on and -off spectra spinning at

DOI: 10.1021/acs.jpcb.7b07213
J. Phys. Chem. B XXXX, XXX, XXX−XXX

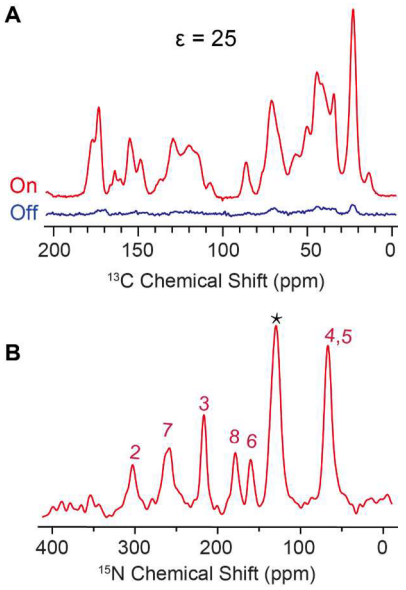

Figure 8. DNP-enhanced (A) ^{13}C and (B) ^{15}N CP-MAS spectra of natural abundance posaconazole-deuterated vinyl acetate ASD. Both experiments were conducted with $\omega_r/2\pi$ = 9 kHz. The enhancement value dependence on spinning frequency is presented in Figure S5. The ^{13}C spectrum was recorded with 128 scans, recycle delay of 10 s. The ^{15}N spectrum was acquired with 1024 scans, recycle delay of 4 s.

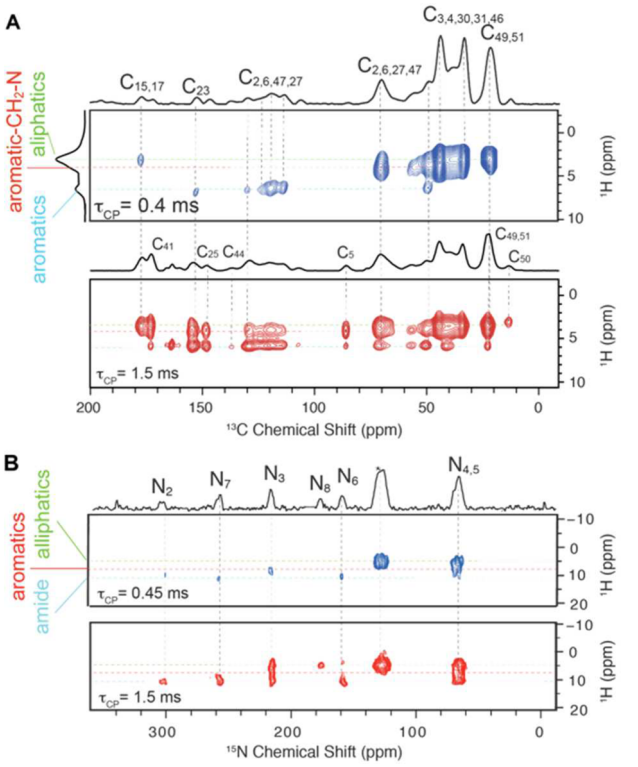

Figure 9. 2D DNP-enabled heteronuclear correlation spectra of natural abundance posaconazole-^2H vinyl acetate ASD: (A) $^{13}C-^1H$ and (B) $^{15}N-^1H$ spectra with short and long mixing times. HETCOR pulse sequence is shown in Figure S2. Each HETCOR experiment was acquired in 7 h at 106 K with 3 s recycle delay, 64 t_1 increments, and 256 scans per increment at $\omega_r/2\pi$ = 9 kHz. The $^{13}C-^1H$ and $^{15}N-^1H$ HETCOR spectra were acquired with FSLG homonuclear decoupling at 400 and 600 MHz, respectively.

9 kHz in Figure 8A. Previous studies have suggested the enhancement dependence on MAS frequencies.[10,64,65] Further optimization exhibited a maximum enhancement of 32 at $\omega_r/2\pi$ = 5 kHz, as shown in Figure S7. Compared to clotrimazole/^2H-vinyl acetate, higher DNP enhancement was achieved for posaconazole/^2H-vinyl acetate ASD, likely due to differing molecular interactions and packings between radicals and APIs. Deuteration of the polymer not only improves the enhancement by a factor of 3−4, but also simplifies the analysis of API signals by suppressing signals originated from the polymer. The ^{15}N spectrum in Figure 8B was acquired in 1 h, while without DNP enhancement, it would have taken almost a month to achieve the comparable sensitivity for the same amount of samples. All eight ^{15}N atoms in the drug molecule can be seen and tentatively assigned according to previous publications.[63] To complete the resonance assignments and establish the intramolecular correlations, 2D heteronuclear experiments were conducted as illustrated in Figure 9.

Pharmaceutical solids are often disordered and multicomponent systems, leading to low resolution in spectroscopic investigations. To obtain unambiguous and high-resolution information for structural elucidations, it is best to use 2D MAS NMR techniques to establish intra- and intermolecular correlations. However, multidimensional correlation becomes extremely challenging and often practically infeasible for low-γ spins, such as ^{13}C and ^{15}N rich drug molecules. DNP-enhanced ^{13}C- and ^{15}N-detected correlation experiments were performed as shown in Figure 9A and B, respectively. Taking 2D $^{13}C-^1H$ HETCOR in Figure 9A, for example, the spectra were collected with 0.4 ms contact times for correlations of short distances and 1.5 ms for long distances. In the ^1H dimension, three types of functional groups including aliphatic, aromatic-N, and aromatic protons can be assigned. At the short mixing time (blue), the cross peaks between adjacent protons and carbon are observed, e.g., cross peaks between C3, 4, 30, 31 and aliphatic protons; C18, 19 and aromatic protons. Giving a longer spin diffusion transfer (red), $^{13}C-^1H$ cross peaks of those at a farther distance appear, e.g., aliphatic C27 and aromatic protons. Distance information is encoded in these correlations at short and long diffusion times, facilitating the assignments of most carbons.[62]

2D $^1H-^{15}N$ HETCOR spectra were also acquired at short (0.45 ms) and long (1.5 ms) mixing times (Figure 9B). Cross peaks are observed between all eight nitrogen atoms and their neighboring protons including aliphatic, aromatic, and amide protons. Given the fact that ^{15}N has lower γ (−4.316 MHz/T) and natural abundance (0.368%) among the spins of interest in pharmaceutical molecules, it is worth emphasizing the success of acquiring these 2D spectra in 7 h, a reasonably short period of time for practical analysis. These results have shown DNP as a powerful technique for enhancing ssNMR signal intensities for investigating structures and probing interactions of natural abundance drugs and formulations.

CONCLUSION

In summary, our study has served as the first documented example of an in situ preparation of DNP samples to support structural investigations of practical formulation processes. Polarizing radicals have been successfully incorporated during routine pharmaceutical production of solid dispersions including SD and HME. The DNP enhancement has been optimized by investigating the sample and its relaxation parameters. Partial deuteration of ASDs results in more than a 3-fold increase in enhancement value. An optimum

DOI: 10.1021/acs.jpcb.7b07213
J. Phys. Chem. B XXXX, XXX, XXX−XXX

enhancement of 20−30 was obtained and enables detection of low drug loading (i.e., 1%) formulations and the 2D homonuclear $^{13}C-^{13}C$ and heteronuclear $^{13}C-^{1}H$ and $^{15}N-^{1}H$ correlations for structural investigations of pharmaceutical formulations.

■ ASSOCIATED CONTENT

Supporting Information

The Supporting Information is available free of charge on the ACS Publications website at DOI: 10.1021/acs.jpcb.7b07213.

DNP enhanced microwave -on and -off spectra of clotrimzaole-copovidone ASD at drug loadings of 1% and 20%; pulse sequences; EPR characterization of radicals in CLT-copovidone ASDs; ^{13}C CP-MAS spectra of Posaconazole-PVP ASD doped with 0, 1, and 2% TOTAPOL; X-ray powder diffraction patterns of crystalline and amophours posaconzaole, PVP, and posaconazole-PVP ASD doped with 0, 1, and 2% TOTAPOL; and full spectrum of $^{13}C-^{13}C$ refocused INADEQUATE of Clotrimazole doped (PDF)

■ AUTHOR INFORMATION

Corresponding Authors

*rgg@mit.edu.

*yongchao.su@merck.com.

ORCID

Robert G. Griffin: 0000-0003-1589-832X

Notes

The authors declare no competing financial interest.

■ ACKNOWLEDGMENTS

This research was supported by Merck-MIT scientific collaboration funding to R.G.G. and Y.S., and by National Institute of Health Grants EB-002804, EB-002026, EB004866, and EB001965. We thank Drs. Christy George and Melanie Rosay (Bruker BioSpin, U.S.) and Dr. Chad Brown and Merck colleagues (Merck Research Laboratories, U.S.) for insightful discussions. We are grateful to members of Richard J. Temkin's group (PSFC, MIT) and members at FBML for their support with the gyrotron and NMR instrumentation.

■ REFERENCES

(1) Paudel, A.; Geppi, M.; Van den Mooter, G. Structural and Dynamic Properties of Amorphous Solid Dispersions: The Role of Solid-State Nuclear Magnetic Resonance Spectroscopy and Relaxometry. *J. Pharm. Sci.* **2014**, *103*, 2635−2662.

(2) Pham, T. N.; Watson, S. A.; Edwards, A. J.; Chavda, M.; Clawson, J. S.; Strohmeier, M.; Vogt, F. G. Analysis of Amorphous Solid Dispersions Using 2D Solid-State NMR and ^{1}H T_1 Relaxation Measurements. *Mol. Pharmaceutics* **2010**, *7*, 1667−1691.

(3) Nie, H.; Su, Y.; Zhang, M.; Song, Y.; Leone, A.; Taylor, L. S.; Marsac, P. J.; Li, T.; Byrn, S. R. Solid-State Spectroscopic Investigation of Molecular Interactions between Clofazimine and Hypromellose Phthalate in Amorphous Solid Dispersions. *Mol. Pharmaceutics* **2016**, *13*, 3964−3975.

(4) Zencirci, N.; Griesser, U. J.; Gelbrich, T.; Apperley, D. C.; Harris, R. K. Crystal Polymorphs of Barbital: News About a Classic Polymorphic System. *Mol. Pharmaceutics* **2014**, *11*, 338−350.

(5) Watts, A. E.; Maruyoshi, K.; Hughes, C. E.; Brown, S. P.; Harris, K. D. M. Combining the Advantages of Powder X-Ray Diffraction and NMR Crystallography in Structure Determination of the Pharmaceutical Material Cimetidine Hydrochloride. *Cryst. Growth Des.* **2016**, *16*, 1798−1804.

(6) Griffin, J. M.; Martin, D. R.; Brown, S. P. Distinguishing Anhydrous and Hydrous Forms of an Active Pharmaceutical Ingredient in a Tablet Formulation Using Solid-State NMR Spectroscopy. *Angew. Chem., Int. Ed.* **2007**, *46*, 8036−8038.

(7) Tatton, A. S.; Pham, T. N.; Vogt, F. G.; Iuga, D.; Edwards, A. J.; Brown, S. P. Probing Intermolecular Interactions and Nitrogen Protonation in Pharmaceuticals by Novel 15N-edited and 2D 14N-1H Solid-State NMR. *CrystEngComm* **2012**, *14*, 2654−2659.

(8) Su, Y.; Andreas, L.; Griffin, R. G. Magic Angle Spinning NMR of Proteins: High-Frequency Dynamic Nuclear Polarization and 1H Detection. *Annu. Rev. Biochem.* **2015**, *84*, 465−497.

(9) Ni, Q. Z.; Daviso, E.; Can, T. V.; Markhasin, E.; Jawla, S. K.; Swager, T. M.; Temkin, R. J.; Herzfeld, J.; Griffin, R. G. High Frequency Dynamic Nuclear Polarization. *Acc. Chem. Res.* **2013**, *46*, 1933.

(10) Can, T. V.; Ni, Q. Z.; Griffin, R. G. Mechanisms of Dynamic Nuclear Polarization in Insulating Solids. *J. Magn. Reson.* **2015**, *253*, 23−35.

(11) Can, T. V.; Walish, J. J.; Swager, T. M.; Griffin, R. G. Time Domain DNP with the Novel Sequence. *J. Chem. Phys.* **2015**, *143*, 054201.

(12) Barnes, A. B.; De Paëpe, G.; Van der Wel, P. C. A.; Hu, K.-N.; Joo, C.-G.; Bajaj, V. S.; Mak-Jurkauskas, M. L.; Sirigiri, J. R.; Herzfeld, J.; Temkin, R. J.; et al. High-Field Dynamic Nuclear Polarization for Solid and Solution Biological NMR. *Appl. Magn. Reson.* **2008**, *34*, 237−263.

(13) Lee, D.; Hediger, S.; De Paëpe, G. Is Solid-State NMR Enhanced by Dynamic Nuclear Polarization? *Solid State Nucl. Magn. Reson.* **2015**, *66−67*, 6−20.

(14) Smith, A. N.; Long, J. R. Dynamic Nuclear Polarization as an Enabling Technology for Solid State Nuclear Magnetic Resonance Spectroscopy. *Anal. Chem.* **2016**, *88*, 122−132.

(15) Ravera, E.; Corzilius, B.; Michaelis, V. K.; Luchinat, C.; Griffin, R. G.; Bertini, I. DNP-Enhanced MAS NMR of Bovine Serum Albumin Sediments and Solutions. *J. Phys. Chem. B* **2014**, *118*, 2957−2965.

(16) Becker-Baldus, J.; Bamann, C.; Saxena, K.; Gustmann, H.; Brown, L. J.; Brown, R. C. D.; Reiter, C.; Bamberg, E.; Wachtveitl, J.; Schwalbe, H.; et al. Enlightening the Photoactive Site of Channelrhodopsin-2 by DNP-Enhanced Solid-State NMR Spectroscopy. *Proc. Natl. Acad. Sci. U. S. A.* **2015**, *112*, 9896−9901.

(17) Smith, A. N.; Caporini, M. A.; Fanucci, G. E.; Long, J. R. A Method for Dynamic Nuclear Polarization Enhancement of Membrane Proteins. *Angew. Chem., Int. Ed.* **2015**, *54*, 1542−1546.

(18) Daube, D.; Aladin, V.; Heiliger, J.; Wittmann, J. J.; Barthelmes, D.; Bengs, C.; Schwalbe, H.; Corzilius, B. Heteronuclear Cross-Relaxation under Solid-State Dynamic Nuclear Polarization. *J. Am. Chem. Soc.* **2016**, *138*, 16572−16575.

(19) Hoff, D. E.; Albert, B. J.; Saliba, E. P.; Scott, F. J.; Choi, E. J.; Mardini, M.; Barnes, A. B. Frequency Swept Microwaves for Hyperfine Decoupling and Time Domain Dynamic Nuclear Polarization. *Solid State Nucl. Magn. Reson.* **2015**, *72*, 79−89.

(20) Cheng, C. Y.; Han, S. I., Dynamic Nuclear Polarization Methods in Solids and Solutions to Explore Membrane Proteins and Membrane Systems. *Annu. Rev. Phys. Chem.*; Johnson, M. A.; Martinez, T. J., Eds.; Annual Reviews: Palo Alto, 2013; Vol. *64*, pp 507−532.

(21) Wang, T.; Park, Y. B.; Caporini, M. A.; Rosay, M.; Zhong, L. H.; Cosgrove, D. J.; Hong, M. Sensitivity-Enhanced Solid-State NMR Detection of Expansin's Target in Plant Cell Walls. *Proc. Natl. Acad. Sci. U. S. A.* **2013**, *110*, 16444−16449.

(22) Kobayashi, T.; Perras, F. A.; Slowing, I. I.; Sadow, A. D.; Pruski, M. Dynamic Nuclear Polarization Solid-State NMR in Heterogeneous Catalysis Research. *ACS Catal.* **2015**, *5*, 7055−7062.

(23) Kubicki, D. J.; Rossini, A. J.; Purea, A.; Zagdoun, A.; Ouari, O.; Tordo, P.; Engelke, F.; Lesage, A.; Emsley, L. Amplifying Dynamic Nuclear Polarization of Frozen Solutions by Incorporating Dielectric Particles. *J. Am. Chem. Soc.* **2014**, *136*, 15711−15718.

(24) Rossini, A. J.; Widdifield, C. M.; Zagdoun, A.; Lelli, M.; Schwarzwalder, M.; Coperet, C.; Lesage, A.; Emsley, L. Dynamic

DOI: 10.1021/acs.jpcb.7b07213
J. Phys. Chem. B XXXX, XXX, XXX−XXX

Nuclear Polarization Enhanced NMR Spectroscopy for Pharmaceutical Formulations. *J. Am. Chem. Soc.* **2014**, *136*, 2324−2334.
(25) Mak-Jurkauskas, M. L.; Bajaj, V. S.; Hornstein, M. K.; Belenky, M.; Griffin, R. G.; Herzfeld, J. Gradual Winding of the Bacteriorhodopsin Chromophore in the First Half of Its Ion-Motive Photocycle: A Dynamic Nuclear Polarization Enhanced Solid State NMR Study. *Proc. Natl. Acad. Sci. U. S. A.* **2008**, *105*, 883−888.
(26) Mollica, G.; Dekhil, M.; Ziarelli, F.; Thureau, P.; Viel, S. Quantitative Structural Constraints for Organic Powders at Natural Isotopic Abundance Using Dynamic Nuclear Polarization Solid-State NMR Spectroscopy. *Angew. Chem., Int. Ed.* **2015**, *54*, 6028−6031.
(27) Pump, E.; Viger-Gravel, J.; Abou-Hamad, E.; Samantaray, M. K.; Hamzaoui, B.; Gurinov, A.; Anjum, D. H.; Gajan, D.; Lesage, A.; Bendjeriou-Sedjerari, A.; et al. Reactive Surface Organometallic Complexes Observed Using Dynamic Nuclear Polarization Surface Enhanced NMR Spectroscopy. *Chem. Sci.* **2017**, *8*, 284−290.
(28) Märker, K.; Paul, S.; Fernández-de-Alba, C.; Lee, D.; Mouesca, J.-M.; Hediger, S.; De Paëpe, G. Welcoming Natural Isotopic Abundance in Solid-State NMR: Probing Π-Stacking and Supramolecular Structure of Organic Nanoassemblies Using DNP. *Chem. Sci.* **2017**, *8*, 974.
(29) Ni, Q. Z.; Markhasin, E.; Can, T. V.; Corzilius, B.; Tan, K. O.; Barnes, A. B.; Daviso, E.; Su, Y.; Herzfeld, J.; Griffin, R. G. Peptide and Protein Dynamics and Low-Temperature/DNP Magic Angle Spinning NMR. *J. Phys. Chem. B* **2017**, *121*, 4997−5006.
(30) Veinberg, S. L.; Johnston, K. E.; Jaroszewicz, M. J.; Kispal, B. M.; Mireault, C. R.; Kobayashi, T.; Pruski, M.; Schurko, R. W. Natural Abundance N-14 and N-15 Solid-State NMR of Pharmaceuticals and Their Polymorphs. *Phys. Chem. Chem. Phys.* **2016**, *18*, 17713−17730.
(31) Elisei, E.; Filibian, M.; Carretta, P.; Colombo Serra, S.; Tedoldi, F.; Willart, J. F.; Descamps, M.; Cesaro, A. Dynamic Nuclear Polarization of a Glassy Matrix Prepared by Solid State Mechanochemical Amorphization of Crystalline Substances. *Chem. Commun.* **2015**, *51*, 2080−2083.
(32) Hirsh, D. A.; Rossini, A. J.; Emsley, L.; Schurko, R. W. Cl-35 Dynamic Nuclear Polarization Solid-State NMR of Active Pharmaceutical Ingredients. *Phys. Chem. Chem. Phys.* **2016**, *18*, 25893−25904.
(33) Märker, K.; Pingret, M.; Mouesca, J.-M.; Gasparutto, D.; Hediger, S.; De Paëpe, G. A New Tool for NMR Crystallography: Complete 13C/15N Assignment of Organic Molecules at Natural Isotopic Abundance Using DNP-Enhanced Solid-State NMR. *J. Am. Chem. Soc.* **2015**, *137*, 13796−13799.
(34) Le, D.; Casano, G.; Phan, T. N. T.; Ziarelli, F.; Ouari, O.; Aussenac, F.; Thureau, P.; Mollica, G.; Gigmes, D.; Tordo, P.; et al. Optimizing Sample Preparation Methods for Dynamic Nuclear Polarization Solid-State NMR of Synthetic Polymers. *Macromolecules* **2014**, *47*, 3909−3916.
(35) Ong, T. C.; Mak-Jurkauskas, M. L.; Walish, J. J.; Michaelis, V. K.; Corzilius, B.; Smith, A. A.; Clausen, A. M.; Cheetham, J. C.; Swager, T. M.; Griffin, R. G. Solvent-Free Dynamic Nuclear Polarization of Amorphous and Crystalline Ortho-Terphenyl. *J. Phys. Chem. B* **2013**, *117*, 3040−3046.
(36) Pinon, A. C.; Rossini, A. J.; Widdifield, C. M.; Gajan, D.; Emsley, L. Polymorphs of Theophylline Characterized by DNP Enhanced Solid-State NMR. *Mol. Pharmaceutics* **2015**, *12*, 4146−4153.
(37) Afeworki, M.; Schaefer, J. Mechanism of DNP-Enhanced Polarization Transfer across the Interface of Polycarbonate Polystyrene Heterogeneous Blends. *Macromolecules* **1992**, *25*, 4092−4096.
(38) Qiu, Y. H.; Geoff, Y. C.; Zhang, G. Z. Developing Solid Oral Dosage Forms. *Pharmaceutical Theory and Practice*; Elsevier Science Bv: Amsterdam, 2009; pp 1−943.
(39) Song, C.; Hu, K.-N.; Joo, C.-G.; Swager, T. M.; Griffin, R. G. Totapol: A Biradical Polarizing Agent for Dynamic Nuclear Polarization Experiments in Aqueous Media. *J. Am. Chem. Soc.* **2006**, *128*, 11385−11390.
(40) Sauvee, C.; Rosay, M.; Casano, G.; Aussenac, F.; Weber, R. T.; Ouari, O.; Tordo, P. Highly Efficient, Water-Soluble Polarizing Agents for Dynamic Nuclear Polarization at High Frequency. *Angew. Chem., Int. Ed.* **2013**, *52*, 10858−10861.
(41) Yang, F.; Su, Y.; Zhang, J.; DiNunzio, J.; Leone, A.; Huang, C.; Brown, C. D. Rheology Guided Rational Selection of Processing Temperature to Prepare Copovidone-Nifedipine Amorphous Solid Dispersions Via Hot Melt Extrusion (HME). *Mol. Pharmaceutics* **2016**, *13*, 3494−3505.
(42) Yang, F.; Su, Y.; Zhu, L.; Brown, C. D.; Rosen, L. A.; Rosenberg, K. J. Rheological and Solid-State NMR Assessments of Copovidone/Clotrimazole Model Solid Dispersions. *Int. J. Pharm.* **2016**, *500*, 20−31.
(43) Barnes, A. B.; Nanni, E. A.; Herzfeld, J.; Griffin, R. G.; Temkin, R. J. A 250 GHz Gyrotron with a 3 GHz Tuning Bandwidth for Dynamic Nuclear Polarization. *J. Magn. Reson.* **2012**, *221*, 147−153.
(44) Bajaj, V. S.; Farrar, C. T.; Hornstein, M. K.; Mastovsky, I.; Vieregg, J.; Bryant, J.; Elena, B.; Kreischer, K. E.; Temkin, R. J.; Griffin, R. G. Dynamic Nuclear Polarization at 9T Using a Novel 250 GHz Gyrotron Microwave Source. 2003. *J. Magn. Reson.* **2011**, *213*, 404−409.
(45) Barnes, A. B.; Mak-Jurkauskas, M. L.; Matsuki, Y.; Bajaj, V. S.; Van der Wel, P. C. A.; DeRocher, R.; Bryant, J.; Sirigiri, J. R.; Temkin, R. J.; Lugtenburg, J.; et al. Cryogenic Sample Exchange NMR Probe for Magic Angle Spinning Dynamic Nuclear Polarization. *J. Magn. Reson.* **2009**, *198*, 261−270.
(46) Thurber, K. R.; Tycko, R. Measurement of Sample Temperatures under Magic-Angle Spinning from the Chemical Shift and Spin-Lattice Relaxation Rate of Br-79 in KBr Powder. *J. Magn. Reson.* **2009**, *196*, 84−87.
(47) Mance, D.; Gast, P.; Huber, M.; Baldus, M.; Ivanov, K. L. The Magnetic Field Dependence of Cross-Effect Dynamic Nuclear Polarization under Magic Angle Spinning. *J. Chem. Phys.* **2015**, *142*, 234201.
(48) Yuan, X.; Sperger, D.; Munson, E. J. Investigating Miscibility and Molecular Mobility of Nifedipine-Pvp Amorphous Solid Dispersions Using Solid-State NMR Spectroscopy. *Mol. Pharmaceutics* **2014**, *11*, 329−337.
(49) Takahashi, H.; Fernández-de-Alba, C.; Lee, D.; Maurel, V.; Gambarelli, S.; Bardet, M.; Hediger, S.; Barra, A.-L.; De Paëpe, G. Optimization of an Absolute Sensitivity in a Glassy Matrix During DNP-Enhanced Multidimensional Solid-State NMR Experiments. *J. Magn. Reson.* **2014**, *239*, 91−99.
(50) Hu, K.-N.; Song, C.; Yu, H.-h.; Swager, T. M.; Griffin, R. G. High-Frequency Dynamic Nuclear Polarization Using Biradicals: A Multifrequency EPR Lineshape Analysis. *J. Chem. Phys.* **2008**, *128*, 052302.
(51) Hu, K.-N.; Yu, H.-h.; Swager, T. M.; Griffin, R. G. Dynamic Nuclear Polarization with Biradicals. *J. Am. Chem. Soc.* **2004**, *126*, 10844−10845.
(52) Akbey, Ü.; Franks, W. T.; Linden, A.; Lange, S.; Griffin, R. G.; van Rossum, B.-J.; Oschkinat, H. Dynamic Nuclear Polarization of Deuterated Proteins. *Angew. Chem., Int. Ed.* **2010**, *49*, 7803−7806.
(53) Rosay, M.; Weis, V.; Kreischer, K. E.; Temkin, R. J.; Griffin, R. G. Two-Dimensional C-13-C-13 Correlation Spectroscopy with Magic Angle Spinning and Dynamic Nuclear Polarization. *J. Am. Chem. Soc.* **2002**, *124*, 3214−3215.
(54) Liao, S. Y.; Lee, M.; Wang, T.; Sergeyev, I. V.; Hong, M. Efficient DNP NMR of Membrane Proteins: Sample Preparation Protocols, Sensitivity, and Radical Location. *J. Biomol. NMR* **2016**, *64*, 223−237.
(55) Kiswandhi, A.; Lama, B.; Niedbalski, P.; Goderya, M.; Long, J.; Lumata, L. The Effect of Glassing Solvent Deuteration and Gd^{3+} Doping on C-13 DNP at 5 T. *RSC Adv.* **2016**, *6*, 38855−38860.
(56) Perras, F. A.; Reinig, R. R.; Slowing, I. I.; Sadow, A. D.; Pruski, M. Effects of Biradical Deuteration on the Performance of DNP: Towards Better Performing Polarizing Agents. *Phys. Chem. Chem. Phys.* **2016**, *18*, 65−69.
(57) Lumata, L.; Merritt, M. E.; Kovacs, Z. Influence of Deuteration in the Glassing Matrix on 13c Dynamic Nuclear Polarization. *Phys. Chem. Chem. Phys.* **2013**, *15*, 7032−7035.
(58) Bouleau, E.; Saint-Bonnet, P.; Mentink-Vigier, F.; Takahashi, H.; Jacquot, J.-F.; Bardet, M.; Aussenac, F.; Purea, A.; Engelke, F.;

DOI: 10.1021/acs.jpcb.7b07213
J. Phys. Chem. B XXXX, XXX, XXX−XXX

Hediger, S.; Lee, D.; De Paepe, G. Pushing NMR Sensitivity Limits Using Dynamic Nuclear Polarization with Closed-Loop Cryogenic Helium Sample Spinning. *Chem. Sci.* **2015**, *6*, 6806−6812.
(59) Mittapalli, S.; Mannava, M. K. C.; Khandavilli, U. B. R.; Allu, S.; Nangia, A. Soluble Salts and Cocrystals of Clotrimazole. *Cryst. Growth Des.* **2015**, *15*, 2493−2504.
(60) Lesage, A.; Bardet, M.; Emsley, L. Through-Bond Carbon−Carbon Connectivities in Disordered Solids by NMR. *J. Am. Chem. Soc.* **1999**, *121*, 10987−10993.
(61) Cadars, S.; Sein, J.; Duma, L.; Lesage, A.; Pham, T. N.; Baltisberger, J. H.; Brown, S. P.; Emsley, L. The Refocused Inadequate MAS NMR Experiment in Multiple Spin-Systems: Interpreting Observed Correlation Peaks and Optimising Lineshapes. *J. Magn. Reson.* **2007**, *188*, 24−34.
(62) Zhong, W.; Yang, X.; Tong, W.; Martin, G. E. Structural Characterization of a Novel Degradant of the Antifungal Agent Posaconazole. *J. Pharm. Biomed. Anal.* **2012**, *66*, 40−49.
(63) Hilton, B. D.; Feng, W. Q.; Martin, G. E. Assignment of the N-15 Resonances of the Antifungal Agent Posaconazole. *J. Heterocycl. Chem.* **2011**, *48*, 948−951.
(64) Hu, K. N.; Song, C.; Yu, H. H.; Swager, T. M.; Griffin, R. G. High-Frequency Dynamic Nuclear Polarization Using Biradicals: A Multifrequency Epr Lineshape Analysis. *J. Chem. Phys.* **2008**, *128*, 052302.
(65) Chaudhari, S. R.; Berruyer, P.; Gajan, D.; Reiter, C.; Engelke, F.; Silverio, D. L.; Coperet, C.; Lelli, M.; Lesage, A.; Emsley, L. Dynamic Nuclear Polarization at 40 kHz Magic Angle Spinning. *Phys. Chem. Chem. Phys.* **2016**, *18*, 10616−10622.

DOI: 10.1021/acs.jpcb.7b07213
J. Phys. Chem. B XXXX, XXX, XXX−XXX